

# A multi-functional nine channels full-spectrum light emitting diodes color temperature palette

Jingjing Liang<sup>1,2</sup>, Hui Cao<sup>1,\*</sup>, Donghua Xu<sup>3</sup>, Xiaobing Lu<sup>4,5</sup>, Javid Atai<sup>6</sup>

<sup>1</sup> School of Computer Science (School of Artificial Intelligence), Guangzhou Maritime University, Guangzhou 510725, China

<sup>2</sup> School of Physics and Materials Science, Guangzhou University, Guangzhou 510006, China

<sup>3</sup> Public laboratory center, Guangzhou Maritime University, Guangzhou 510725, China

<sup>4</sup> Department of Nutritional and Metabolic Psychiatry, The Affiliated Brain Hospital of Guangzhou Medical University, Guangzhou 510370, China

<sup>5</sup> Guangdong Engineering Technology Research Center for Translational Medicine of Mental Disorders, Guangzhou 510370, China

<sup>6</sup> School of Electrical and Information Engineering, The University of Sydney, NSW 2006, Australia

\* Corresponding author: Hui Cao, 978739471@qq.com

## CITATION

Liang J, Cao H, Xu D, et al. A multi-functional nine channels full-spectrum light emitting diodes color temperature palette. *Sound & Vibration*. 2024; 59(1): 1722. <https://doi.org/10.59400/sv.v59i1.1722>

## ARTICLE INFO

Received: 9 September 2024

Accepted: 10 October 2024

Available online: 5 November 2024

## COPYRIGHT



Copyright © 2024 by author(s). *Sound & Vibration* is published by Academic Publishing Pte Ltd. This work is licensed under the Creative Commons Attribution (CC BY) license. <https://creativecommons.org/licenses/by/4.0/>

**Abstract:** A multi-functional nine channels full-spectrum light emitting diodes color temperature palette with continuously tunable color temperature at 1 K interval in 2500 K–6500 K, high color rendering of  $R_a > 94$ ,  $R_1-R_{15} > 90$ ,  $R_f > 91$ ,  $96 \leq R_g \leq 104$  is proposed.  $|Duv| < 0.001$  is also achieved. The circadian effect of light source with melanopic efficacy of luminous radiation of 0.6 mW/lm–1.14 mW/lm and circadian action factor of 0.424 blm/lm–0.96blm/lm are obtained. The color temperature palette enables precise control and reproduction of color temperature of sunlight with corresponding circadian effect, which is of positive significance for visual fields such as photography or art exhibitions and regulation of circadian rhythm.

**Keywords:** color temperature palette; full-spectrum; high color rendering; color temperature reproduction; circadian effect

## 1. Introduction

In recent years, full-spectrum lighting has been gradually gaining ground in the lighting market. Due to its excellent color rendering, full-spectrum lighting is ideal for applications where high color rendering is required, such as cinematography, art galleries, exhibitions, etc. [1–3]. With the discovery of intrinsically photosensitive retinal ganglion cells (ipRGCs) [4–7], healthy lighting has been a research hotspot. Full-spectrum light source stands out for their ability to mimic natural light environment and change color temperature based on the time of day. In the era of solid-state lighting, LED has significant advantages such as high efficiency and long life. Combined with the theme of health lighting, full-spectrum lighting LED came into being [8].

Currently, full-spectrum LEDs are mainly developed in two ways: LED chips + phosphors [9] and multi-channel LED chips. Regarding the approach of phosphors + LED chips, in the early days, white LED was mainly achieved by blue LED chip (440 nm–470 nm) with  $Y_3Al_5O_{12}:Ce^{3+}$  yellow phosphor and near-ultraviolet (n-UV) chip + tricolor phosphor (red + green + blue) with blue chip + green + red phosphor [10–14]. However, there was a problem of “cyan gap” [15]. Therefore, the development of a new phosphor emitting in the blue-cyan region has become a research priority [16–18]. Nevertheless, there are some deficiencies with this

approach, such as low quantum conversion efficiency of the phosphor, harsh conditions for cyan phosphor production as well as thermal quenching, water resistance and thermal stability.

As for the approach based on multi-channel LED chips, this method has two advantages: high luminous efficiency and flexible color temperature regulation. Since the multi-channel white LEDs are directly driven by the current through each LED chip, there is no energy loss caused by Stokes shift and non-radiative recombination, which means its energy dissipation is very low, resulting in high luminous efficiency. Also, they can be adjusted by varying the current of different LED chips to control the chromaticity, color temperature or other characteristics. Even the color temperature can be set to be tunable within a specific range [19–23]. However, according to the previous studies, the tunable switching points of color temperature were few and discontinuous. Light sources that have color temperature smoothly adjusted over 1 K interval on the basis of tunable color temperature are still rare, not to mention maintaining high color rendering and non-visual effects while keeping the color temperature tunable at 1 K interval. To achieve high quality illumination, a light source that has excellent color rendering with a minimum requirement of color rendering index (CRI) being greater than 90 is needed. A small Duv is also required. The short-wave blue light can cause damage to the retina, which will lead to circadian rhythm disorders [24–27]. Therefore, in the design of the spectrum, it is necessary that the proportion of harmful blue light should not be too large. With the discovery of the non-visual effects of light, full-spectrum light sources that mimic the color temperature variations of sunlight throughout the day helping regulating the circadian rhythm are also very promising.

In this paper, A multi-functional nine channels full-spectrum LEDs color temperature palette is proposed with continuously tunable color temperature at 1 K interval in 2500 K–6500 K compared to the common four-channel [19], five-channel [23] and six-channel LEDs [20] and it enables precise control and reproduction of color temperature variations of sunlight. By traversing the luminous flux ratios of nine LEDs, the high color rendering index (CRI) inclusion of Duv is obtained. In addition to reproduce the color temperature variations of sunlight, a corresponding non-visual effect of light source is also wanted, so that it can be similar to sunlight in both visual and non-visual way and better regulate the human body's rhythms. Therefore, the parameters of non-visual effect of melanopic efficacy of luminous radiation (MELR) [22] and circadian action factor (CAF) [20] are optimized according to the maximal and minimal MELR values for the considered Rf constraints [28] and characteristics of light at different time of the day.

## 2. Materials and methods

Multi-channel LED follows the principle of linear superposition of spectrum. The overall spectral power distributions (SPDs) consist of the SPD of each individual LED chip, which can be expressed as follows:

$$S(\lambda) = L_1 \cdot S_1(\lambda) + L_2 \cdot S_2(\lambda) + L_3 \cdot S_3(\lambda) + \dots + L_n \cdot S_n(\lambda) \quad (1)$$

where  $\lambda \in [380, 780]$ ,  $n \in [1, 9]$ ;  $S(\lambda)$ ,  $L_n$  and  $S_n(\lambda)$  denote the overall spectral

power distribution, the luminous flux ratio and the spectral power distribution of the  $n$ -th monochromatic LED, respectively.  $\lambda_o$  is the peak wavelength of LED. We assume that the SPD of the  $n$ th monochromatic LED follows the Gaussian distribution [29], which can be expressed by:

$$S_n(\lambda) = \frac{1}{\sigma\sqrt{2\pi}} e^{-\frac{1}{2}\left(\frac{\lambda-\lambda_o}{\sigma}\right)^2} \quad (2)$$

where  $\sigma$  is the standard deviation associated with the full width half maximum (FWHM) as  $\Delta\lambda = 2\sigma\sqrt{2\ln 2}$ .

The reason we chose nine LED channels is that selecting three “dots” (one dot corresponds to one channel) each in the red, green and blue color bands of 380 nm–780 nm allows for good continuity of the spectrum. The more “dots” are selected, The more continuous and colorful the final combined spectrum becomes. The corresponding peak wavelength and FWHM of nine LEDs were summarized in **Table 1**. The normalised spectral power distribution of nine LEDs was shown in **Figure 1**.

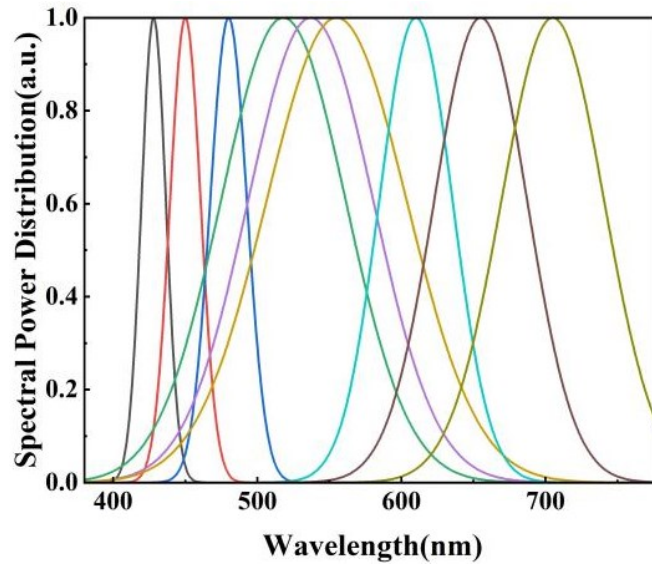


**Figure 1.** Normalised spectral power distribution curves for nine LEDs.

In **Table 1**, the wavelength of 425 nm, 450 nm, 480 nm are more sensitive to the human eye and therefore were adjusted to the smallest FWHM. 480 nm is beneficial to regulation of circadian rhythm. Compared to 480 nm, 425 nm and 450 nm are somehow harmful to the human eye but they are indispensable components of visual processes, therefore their FWHM have been adjusted to be smaller than the FWHM of 480 nm. The wavelength of 518 nm, 537 nm, 555 nm belongs to the comfort region of the human eye hence their FWHM wavelength are set to be the largest. The wavelength of 610 nm, 655 nm, 705 nm belongs to the red-light region, which are also indispensable components of visual processes and beneficial for human skin so their FWHM are set to be the second largest.

**Table 1.** Nine LEDs of peak wavelength  $\lambda_0$  and full width at half maxima  $\Delta\lambda$ .

LED	$\lambda_0/\text{nm}$	$\Delta\lambda/\text{nm}$
Purple	425	20
Indigo	450	25
Blue	480	30
Green	518	102
Yellow green-1	537	102.3
Yellow green-2	555	114.5
Orange	610	60
Red-1	655	76
Red-2	705	84

In terms of the visual effect of light source, the small sample size of CRI standard makes it somewhat flawed [30] while TM-30 has a larger sample size and takes into account color fidelity and saturation, making it a more rigorous criterion for evaluating color quality. Consider that CRI standard is still somewhat representative, the CRI and TM-30 standards were combined to comprehensively evaluate the color rendering of light source. Duv and CCT were introduced to evaluate the chromaticity performance of the light source. By adjusting these two parameters, the chromaticity coordinate of the light source can be as close as possible to the blackbody Planck's curve. In terms of the non-visual effect of light source, MELR and CAF were optimized according to the maximal and minimal MELR values for the considered Rf constraints and characteristics of light at different time of the day. High MELR can inhibit the secretion of melatonin. Low MELR can reduce the inhibitory effect of melatonin secretion. High CAF refers to high concentration of radiant energy of blue light. Low CAF refers to low concentration of blue light. Therefore, larger MELR and CAF are needed at midday and smaller MELR and CAF are needed at night fall, while medium MELR and CAF are needed in early morning and afternoon.

Next, regarding the visual and non-visual optimization of the light source, the corresponding functions were introduced:  $F_{\text{CRI}}$ ,  $F_{\text{Rf}}$ ,  $F_{\text{Rg}}$ ,  $F_{\text{Duv}}$ ,  $F_{\text{MELR}}$  [22],  $F_{\text{CAF}}$  [20]. The mathematical expressions of CRI, Rg, Rf are complex, and can be consulted in GB/T 5702-2019 Color Rendering Evaluation Method of light source and ANSI/IES TM-30-20 (IES 2020), which will not be detailed here. The mathematical expressions of the rest functions can be expressed as follows.

$$F_{\text{CCT}} = 669M^4 - 779M^3 + 3360M^2 - 7047M + 5652, M = \frac{x - 0.329}{y - 0.187} \quad (3)$$

$$F_{\text{Duv}} = \left( \frac{|k \times u - v + v_0 - k \times u_0|}{(k^2 + 1)^{\frac{1}{2}}} \right) \text{sign}(v - v_0), k = \frac{v - v_0}{u - u_0} \quad (4)$$

$$F_{\text{MELR}} = \frac{\int_{380}^{780} S(\lambda) \text{smel}(\lambda) d\lambda}{K_m \int_{380}^{780} S(\lambda) d\lambda} \quad (5)$$

$$F_{CAF} = \frac{\int_{380}^{780} S(\lambda) C(\lambda) d\lambda}{K_m \int_{380}^{780} S(\lambda) V(\lambda) d\lambda} \quad (6)$$

where  $M$  denotes  $(x - 0.329)/(y - 0.187)$ ,  $k$  denotes  $(v - v_o)/(u - u_o)$ ,  $x$  and  $y$  denotes the CIE 1931 color coordinate of the light source.  $u$ ,  $v$ ,  $u_o$ ,  $v_o$  denote the CIE 1960 chromaticity coordinates of the light source and Planck's Blackbody, respectively.  $S(\lambda)$  denotes the spectral power distribution.  $Smel(\lambda)$  is the melanoptic action spectra.  $K_m$  is the maximum spectral luminous efficacy of the radiation for photopic vision.  $K_m = 683 \text{ lm/W}$ .  $C(\lambda)$  denotes the spectral circadian efficiency.  $V(\lambda)$  is the spectral luminous efficiency function for photopic vision.

Firstly, the visual aspect of the light source was optimized subject to the following constraints in order to achieve excellent chromaticity and high color rendering of the light source:

$$\begin{cases} F_{CCT}(\lambda) \in [2700, 6500], |F_{Duv}(\lambda)| \leq 0.001 \\ F_{CRI}(\lambda) \geq 90, F_{Rf}(\lambda) \geq 90, 90 \leq F_{Rg}(\lambda) \leq 110 \end{cases} \quad (7)$$

Secondly, the non-visual aspect of the light source was optimized based on the following constraints.  $G_{time}$  denotes the desired spectrum of different time of the day. According to maximal and minimal MELR values for the considered Rf constraints as well as the characteristics of different time of a day: at midday, the MELR and CAF were required to be as large as possible, while at night fall the MELR and CAF were required to be as low as possible. In the morning or afternoon, MELR and the CAF were required to be medium between the values at night fall and midday, the following constraints were introduced:

$$\begin{cases} G_{midday} = \text{MAX} \{F_{MELR}(\lambda), F_{CAF}(\lambda)\} \\ G_{night\ fall} = \text{MIN} \{F_{MELR}(\lambda), F_{CAF}(\lambda)\} \\ G_{morning/afternoon} = \text{MEDIUM} \{F_{MELR}(\lambda), F_{CAF}(\lambda)\} \\ MELR_{night\ fall} \in [0.4, 0.9]; \\ MELR_{morning/afternoon} \in [0.6, 1.2] \\ MELR_{midday} \in [0.8, 1.4] \end{cases} \quad (8)$$

Next, the above theoretical model will be simulated to verify its reliability. Here, MATLAB will be used for simulation. The optimization process consists of six steps as which are shown in **Figure 2**. The following settings in step 1 will be taken to optimize the calculation process and improve the efficiency of the algorithm. Based on the Gaussian monochromatic LED model and multi-channel LED mixing technology, nine "steps" are set between 0 and 1: 0.01, 0.13, 0.25, 0.38, 0.50, 0.62, 0.74, 0.87, 1. The energy ratio of the nine LEDs L1–L9 are traversed according to the set step value. In addition, for 2700 K–5000 K, the weights of 555 nm, 610, 655, 705 nm channels are set to be 2, 2, 4 and 8 times greater, respectively, and for 5000 K–6000 K, the weights of all channels are 1.

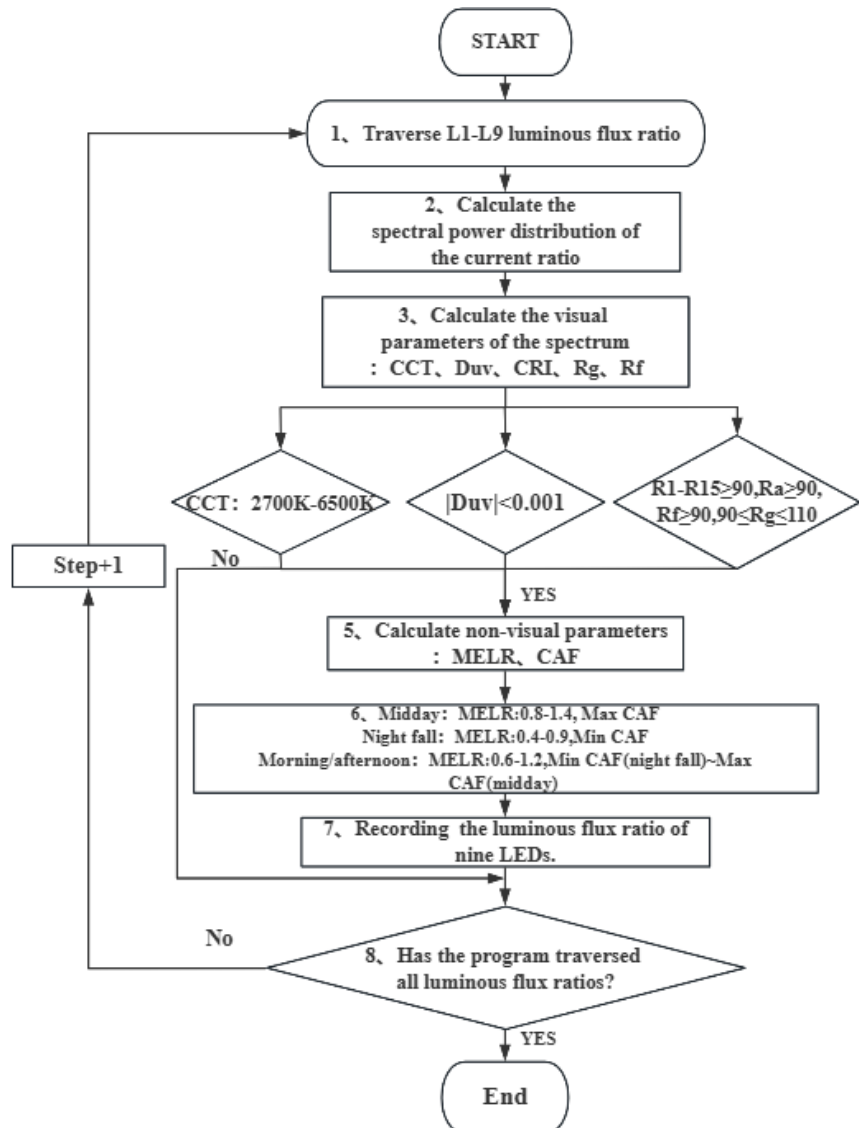
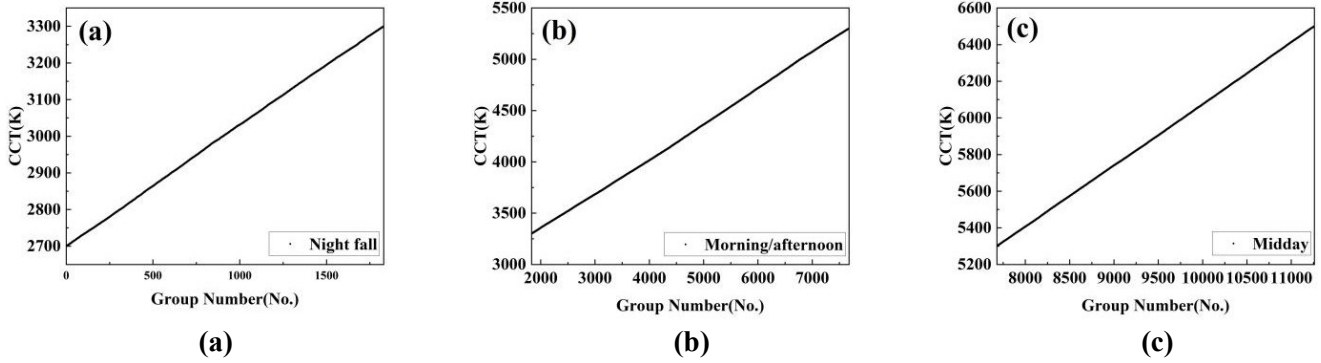


Figure 2. Spectral optimization flowchart.

### 3. Result and discussion

Through simulations, the spectrum cluster of 2700 K–6500 K have obtained. Generally speaking, given the characteristics of different time of the day, the color temperature of the night fall, morning/afternoon, midday correspond to the range of 2700 K–3300 K, 3300 K–5300 K and 5300 K–6500 K, respectively. The luminous flux ratios of nine LEDs of spectrum cluster were collected. A set of luminous flux ratios of nine LEDs is taken as a group to correspond to one color temperature. These groups were sorted and numbered in order of color temperature from lowest to highest, so that each group number corresponds to a specific color temperature. The color temperature curves for different time of the day are shown in **Figure 3**. The spectrum cluster at night fall have group numbers ranging from 1 to 1830, while the spectrum cluster in the morning/afternoon have group numbers ranging from 1831 to 7678, and the spectrum cluster at midday have group numbers ranging from 7679 to 11,261. The color temperature can be switched with high precision at 1 K interval and result in a smooth curve. In other words, the high-precision smooth switch of

color temperature can be served as a color temperature palette, which allows us to adjust to any desired color temperature (within 2700 K–6500 K) with high precision and high color rendering. It also ensures no stiff visual change when switching which can provide a high-quality auxiliary tool for photography where a subtle difference in color temperature will lead to a very different visual effect. Likewise, in art exhibitions where high color rendering of light and accurate adjustment of color temperature are also required, the light source can provide a high-quality full-spectrum light source for these kinds of fields.



**Figure 3.** Color temperature curves in different time of the day. **(a)** night fall; **(b)** morning/afternoon; **(c)** midday.

The spectral power distributions of 2700 K–6500 K are shown in **Figure 4a**. The three-dimensional spectral power distribution for night fall, morning/afternoon and midday are shown in **Figure 4b–d**. **Figure 4b** shows that the spectrum at night fall have the highest proportion of red light and the lowest proportion of blue light. As the color temperature increases, the proportion of red light begins to decrease while the proportion of blue light gradually increases, but the increase is small. **Figure 4c** shows that in the morning/afternoon, compared with the spectrum at night fall, the proportion of red light is significantly reduced and the proportion of blue light is further increased. This is due to the fact that appropriate rhythm stimulation is needed in the morning/afternoon to support people’s daily activities. **Figure 4d** demonstrates that in midday, the proportion of blue light reaches the highest and features stronger spikes. It explains why the non-visual parameters MELR and CAF at midday are set to be higher and at night fall are set to be lower.

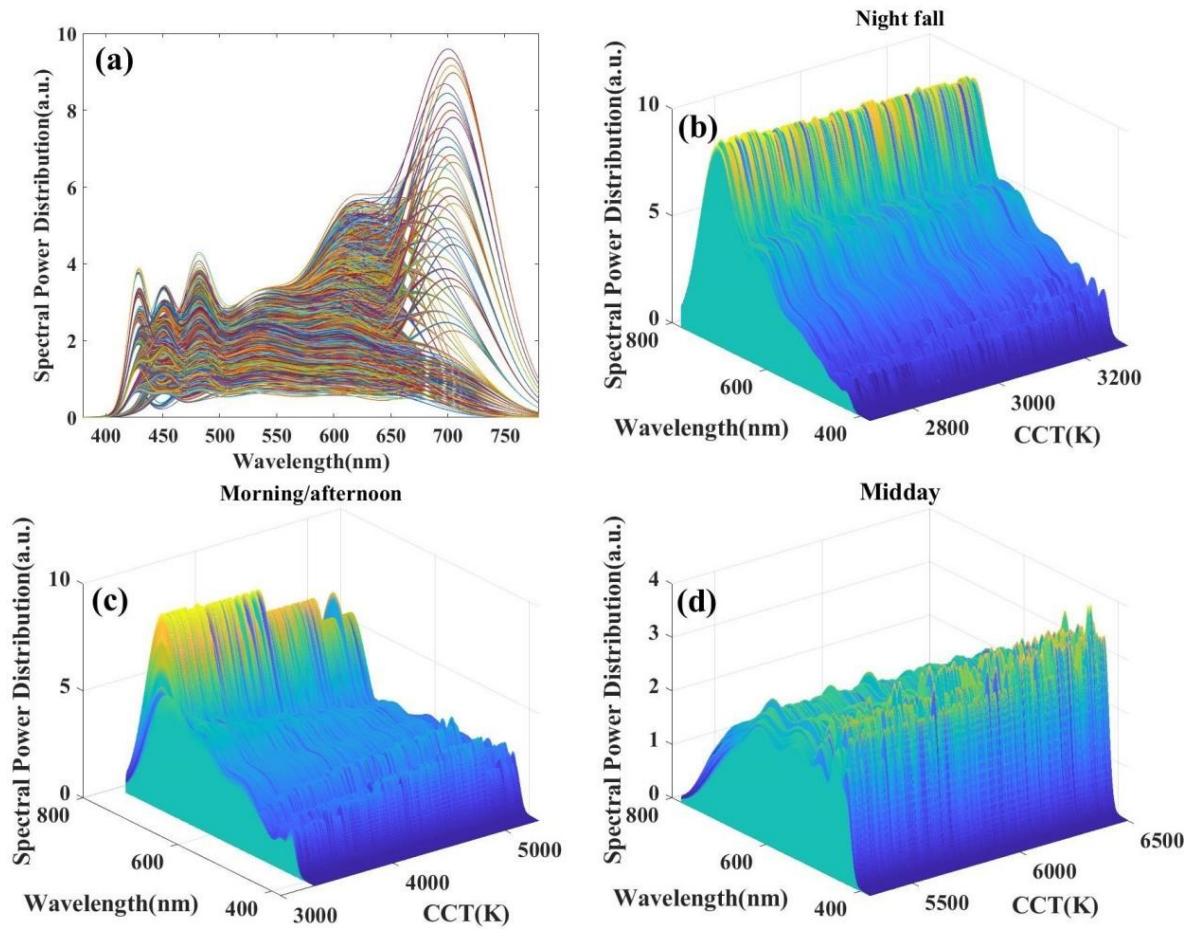


**Figure 4.** Spectral power distribution of 2700 K–6500 K and three-dimensional spectral power distribution in different time of the day. (a) two-dimensional spectral power distribution; (b) night fall; (c) morning/afternoon; (d) midday.

Comparing the spectrum shapes of different time of the day, it can be seen that the shape of the spectrum changes with different time. At midday the spectrum is mainly concentrated in the blue-green light, while at other times in the yellow-red light. The sensory perceptions provided by the light source in different time of the day are as follows: at night fall, users are provided with a comfortable warm white light atmosphere which is closer to the natural light at sunset, allowing people to relax. In the morning/afternoon, users are provided with a softer light and a neutral white light atmosphere which is closer to the natural light in the morning or afternoon, giving people a feeling of serenity. In the midday, users are provided with a cold white light and a transparent, bright, cool atmosphere which is closer to natural midday light, helping people to focus attention. As a result, it can conclude that real-time color temperature reproduction of sunlight outdoors can be achieved indoors by the light source.

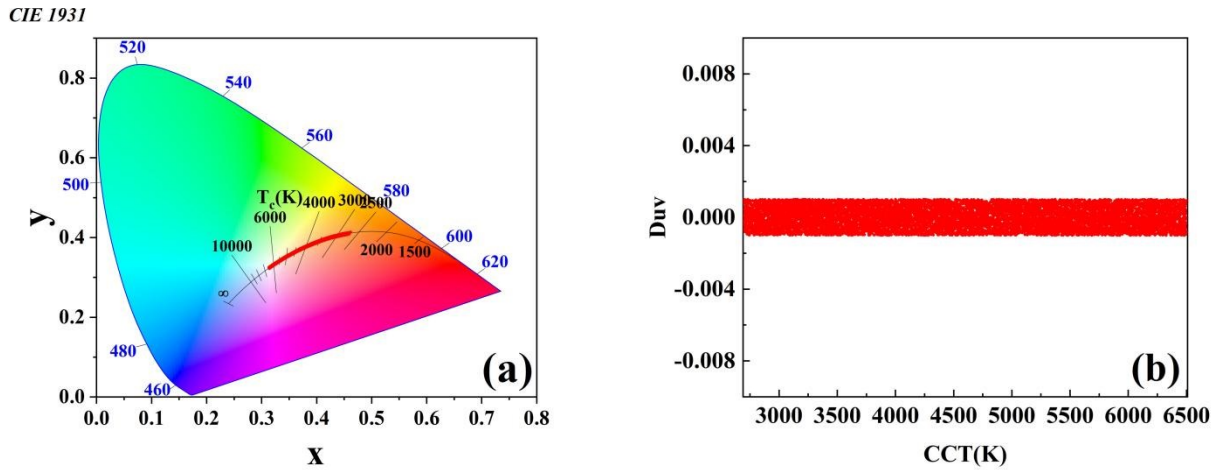


**Figure 5.** CCT and Duv of light source. (a) chromaticity coordinate of 2700 K–6500 K on the CIE 1931 chromaticity diagram; (b) Duv of 2700 K–6500 K.

The chromaticity coordinate on CIE 1931 chromaticity diagram and the Duv of 2700 K–6500 K are shown in **Figure 5**. As is shown in **Figure 5b**, the Duv of 2700 K–6500 K are consistent with  $|Duv| < 0.001$ , well below the threshold of color difference considered perceptible by the human eye. Combined with the chromaticity coordinate in **Figure 5a**, it can conclude that the color temperature of the light source is very close to the corresponding color temperature on the Planck’s blackbody curve. The trajectory of the color temperature is also very similar to the curve of Planck’s blackbody, indicating the excellent chromaticity of the light source.

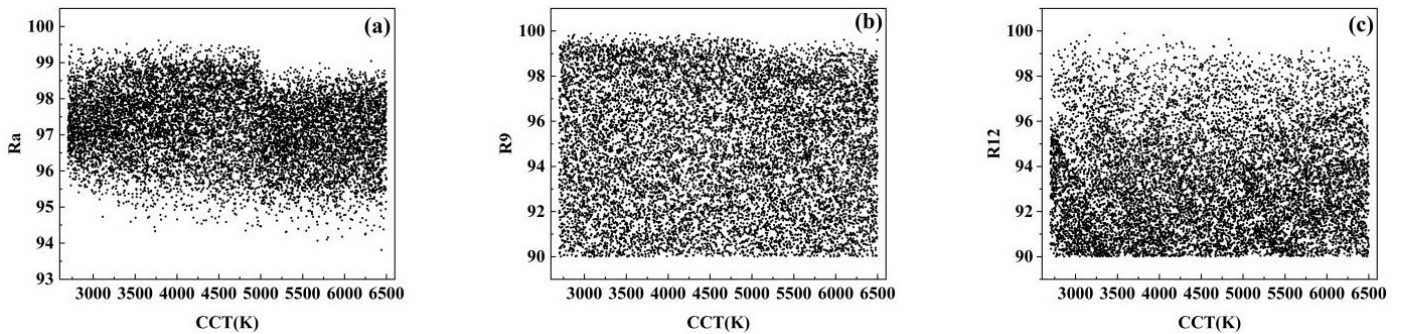


**Figure 6.** CRI of 2700 K–6500 K. (a) Ra; (b) R9; (c) R12.

The CRI of 2700 K–6500 K is shown in **Figure 6**. As we can see, all the color temperature of R1–R15 and Ra are greater than 90. In particular, Ra can reach an average of 97 and an average of 98, 98, 97, 96, 98, 97, 97, 97, 95, 96, 96, 93, 98, 98, 98 for R1–R15. In **Figure 6b,c**, R9 and R12 of the light source can reach above 90.

The fidelity index Rf (horizontal coordinate) and the gamut index Rg (vertical coordinate) of TM-30 color quality evaluation of 2700 K–6500 K are shown in **Figure 7**. According to ANSI/IES TM-30-20 [23], Rf and Rg characterize the degree of similarity and the change in saturation of each standard color under the test light source compared with the reference light source, respectively. The limit of the Planckian light source is denoted by the dashed line and the limit of the actual light

source is denoted by the solid line. The fidelity index  $R_f$  ranges from 0 to 100.  $R_g$ , on the other hand, has no limitation but its value changes with the value of  $R_f$ , and is generally best valued at around 100. Their values are theoretically distributed in the area enclosed by the dashed, solid lines and the coordinate axes. As is shown in **Figure 7**, the  $R_f$  and  $R_g$  of the light source are distributed within the dashed region. The fidelity index of  $R_f \geq 91$ , an average of 96 and the gamut index of  $96 \leq R_g \leq 104$ , and average of 101 are achieved, indicating the low chromatic aberration and appropriate color saturation of the light source. Combining the results of the chromaticity diagram and CRI from **Figures 5** and **6**, it can conclude that a superb color rendering of the light source is attained, which can easily meet the fields with high color rendering requirements.

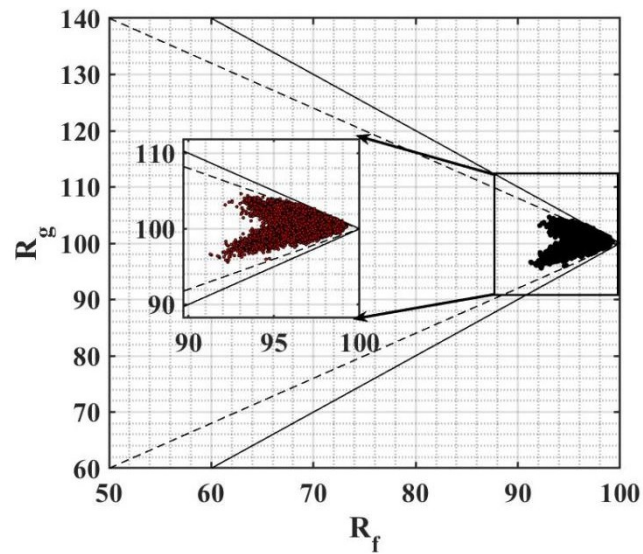


**Figure 7.** Dual evaluation system of  $R_f$  and  $R_g$  for TM-30.

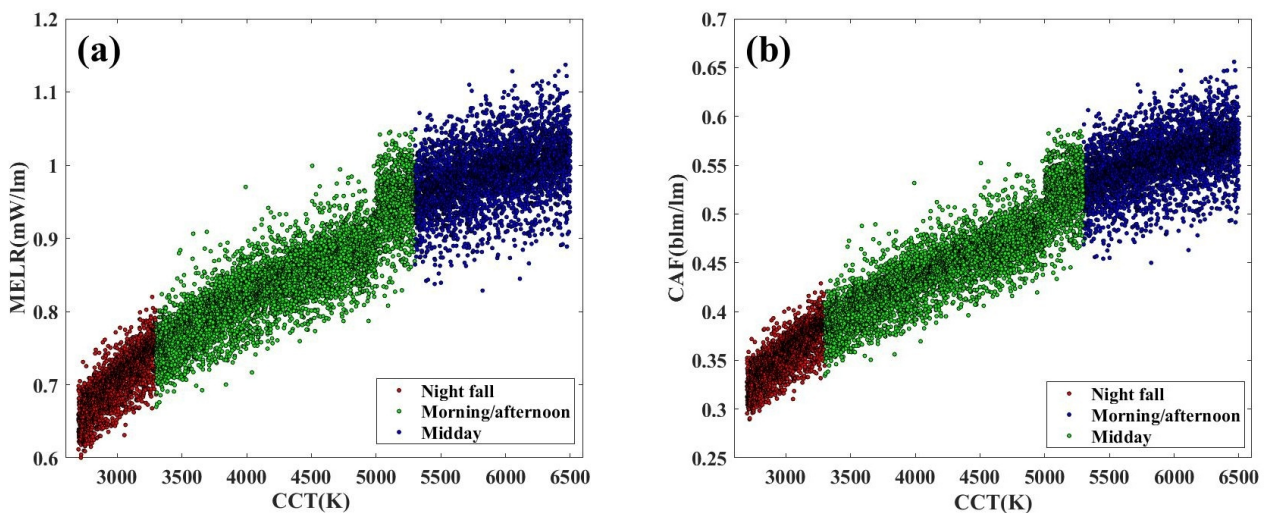


**Figure 8.** The MELR, CAF of different time of the day (red markers denote night fall, green markers denote morning/afternoon, blue markers denote midday). **(a)** MELR; **(b)** CAF.

In order to better mimic sunlight even further, a corresponding non-visual effect of light source is also wanted. The values of MELR, CAF according to different time

of the day are shown in **Figure 8**. The values of MELR and CAF with color temperature are shown in **Figure 8a**, where the red, green and blue parts correspond to night fall, morning/afternoon and midday, respectively. It is noted that MELR and CAF increase as the color temperature is risen. This stems from the fact that the sensitive wavelengths of MELR and CAF are close to blue light region and the proportion of blue light increases with increasing color temperature. As shown in **Figure 8b**, the tunable MELR range of 0.6 mW/lm–1.14 mW/lm and the tunable CAF range of 0.424 blm/lm–0.96blm/lm are attained, both of which can fulfill the basic requirement to regulate the circadian rhythm [25]. It can also be seen that the tunable range of MELR and CAF are different among different time of the day. It is noteworthy that the minimum and maximum of MELR and CAF of different time of the day are increased in turn. It can conclude that the light source can reproduce the color temperature while having corresponding non-visual effects, which can better regulate the circadian rhythm. To sum up, the light source has two modes: in visual mode, it is a full-spectrum light source with continuously tunable CCT; in non-visual mode, the CCT of outdoor sunlight can be reproduced indoors in real time with corresponding circadian rhythm. The multi-functional lighting modes of the light source can be summarized in **Table 2**.

**Table 2.** The multi-functional lighting modes of the light source.

Visual	Ra	Rf	Rg
Full-spectrum	96	97	104
Non-visual	CCT (K)	MELR (mW/lm)	CAF (blm/lm)
Night fall	2700–3300	0.6–0.82	0.424–0.628
Morning/afternoon	3300–5300	0.67–1.05	0.489–0.858
Midday	5300–6500	0.829–1.14	0.659–0.96

#### 4. Conclusion

In this paper, A multi-functional nine channels full-spectrum LEDs color temperature palette with continuously tunable color temperature at 1 K interval in 2500 K–6500 K, high color rendering of  $R_a > 94$ ,  $R_1-R_{15} > 90$ ,  $R_f > 91$ ,  $96 \leq R_g \leq 104$  is proposed.  $|Duv| < 0.001$  and low blue light hazard are also achieved. The circadian effect of light source with melanopic efficacy of luminous radiation of 0.6 mW/lm–1.14 mW/lm and circadian action factor of 0.424 blm/lm–0.96 blm/lm are achieved. The high-precision smooth switch of color temperature of the light source can be serve as a color temperature palette, which allows us to adjust to the desired color temperature and reproduction the color temperature of sunlight with high precision and high color rendering and having corresponding non-visual effects. The multi-functional nine-channel LEDs full-spectrum color temperature palette of this study is of positive significance for the field that requires high color rendering and regulation of circadian rhythm, which paves the way for the development of intelligent and tunable high-quality full-spectrum light source.

**Author contributions:** Methodology, JL and HC; formal analysis, JL and HC; writing—original draft preparation, JL; writing—review and editing, JL, HC, DX,

XL and JA; supervision, HC, JA, DX and XL. All authors have read and agreed to the published version of the manuscript.

**Funding:** Bureau of Education of Guangzhou Municipality(202234641); Department of Education of Guangdong Province(2020ZDZX3072,2021KTSCX098); Research Project of Construction National Science and Technology Think Tank of Guangdong Province (SXK20220201035); Education and Science Program of Guangdong Province (2022GXJK308); Project of Construction Discipline Scientific Research Capability Improvement of Guangdong Province(2022ZDJS098, 2022ZDJS096); Guangzhou Key R&D Program Agriculture and Social Development Science and Technology Project (202206010034) and Guangzhou Municipal Basic Research Project jointly funded by municipal schools (institutes) (2023A03J0834).

**Acknowledgments:** The authors thank the reviewers for their valuable suggestions regarding this work.

**Conflict of interest:** The authors declare no conflict of interest.

## References

1. Liang M, Xu J, Qiang Y, et al. Ce<sup>3+</sup> doped BaLu<sub>2</sub>Al<sub>2</sub>Ga<sub>2</sub>SiO<sub>12</sub>—A novel blue-light excitable cyan-emitting phosphor with ultra-high quantum efficiency and excellent stability for full-spectrum white LEDs. *Journal of Rare Earths*. 2021; 39(9): 1031–1039. doi: 10.1016/j.jre.2020.09.015
2. Wu AH, Wang QT. Application of raman spectroscopy in the lithium battery industry. *Journal of Guangzhou Maritime University*. 2023; 31(04): 55–61.
3. Qin XF, Zhu JS, Sun HY. Construction of the evaluation index system of night navigation ship's bridge light environment. *Journal of Guangzhou Maritime University*. 2023; 31(01): 13–17.
4. Berson DM, Dunn FA, Takao M. Phototransduction by Retinal Ganglion Cells That Set the Circadian Clock. *Science*. 2002; 295(5557): 1070–1073. doi: 10.1126/science.1067262
5. Hatori M, Gronfier C, Van Gelder RN, et al. Global rise of potential health hazards caused by blue light-induced circadian disruption in modern aging societies. *npj Aging and Mechanisms of Disease*. 2017; 3(1). doi: 10.1038/s41514-017-0010-2
6. Oh JH, Yoo H, Park HK, et al. Analysis of circadian properties and healthy levels of blue light from smartphones at night. *Scientific Reports*. 2015; 5(1): 11325. doi: 10.1038/srep11325
7. Wahl S, Engelhardt M, Schaupp P, et al. The inner clock—Blue light sets the human rhythm. *Journal of Biophotonics*. 2019; 12(12). doi: 10.1002/jbio.201900102
8. Chhajed S, Xi Y, Li YL, et al. Influence of junction temperature on chromaticity and color-rendering properties of trichromatic white-light sources based on light-emitting diodes. *Journal of Applied Physics*. 2005; 97(5): 054506. doi: 10.1063/1.1852073
9. Lin CC, Liu RS. Advances in Phosphors for Light-emitting Diodes. *The Journal of Physical Chemistry Letters*. 2011; 2(11): 1268–1277. doi: 10.1021/jz2002452
10. Jiang C, Peng M, Srivastava AM, et al. Brik M. Mn<sup>4+</sup>-Doped Heterodialkyl Fluorogermanate Red Phosphor with High Quantum Yield and Spectral Luminous Efficacy for Warm-White-Light-Emitting Device Application. *Inorganic Chemistry*. 2018; 57(23): 14705–14714. doi: 10.1021/acs.inorgchem.8b02488
11. Wei Y, Xing G, Liu K, et al. New strategy for designing orangish-red-emitting phosphor via oxygen-vacancy-induced electronic localization. *Light: Science & Applications*. 2019; 8(1). doi: 10.1038/s41377-019-0126-1
12. Narukawa Y, Narita J, Sakamoto T, et al. Ultra-High Efficiency White Light Emitting Diodes. *Japanese Journal of Applied Physics*. 2006; 45(10L): L1084. doi: 10.1143/jjap.45.L1084
13. Fukuda Y, Matsuda N, Okada A, et al. White Light-Emitting Diodes for Wide-Color-Gamut Backlight Using Green-Emitting Sr-Sialon Phosphor. *Japanese Journal of Applied Physics*. 2012; 51(12R): 122101. doi: 10.1143/jjap.51.122101

14. Zhang B, Ying S, Wang S, et al. Blue-Green-Yellow Color-Tunable Luminescence of Ce<sup>3+</sup>-, Tb<sup>3+</sup>-, and Mn<sup>2+</sup>-Codoped Sr<sub>3</sub>Y<sub>2</sub>Na(PO<sub>4</sub>)<sub>3</sub>F via Efficient Energy Transfer. *Inorganic Chemistry*. 2019; 58(7): 4500–4507. doi: 10.1021/acs.inorgchem.9b00030
15. Zhao M, Liao H, Molochev MS, et al. Emerging ultra-narrow-band cyan-emitting phosphor for white LEDs with enhanced color rendition. *Light: Science & Applications*. 2019; 8(1). doi: 10.1038/s41377-019-0148-8
16. Liang J, Devakumar B, Sun L, et al. Full-visible-spectrum lighting enabled by an excellent cyan-emitting garnet phosphor. *Journal of Materials Chemistry C*. 2020; 8(14): 4934–4943. doi: 10.1039/d0tc00006j
17. Ishimoto S, Han DP, Yamamoto K, et al. Improvement of emission efficiency with a sputtered AlN buffer layer in GaInN-based green light-emitting diodes. *Japanese Journal of Applied Physics*. 2019; 58(SC): SC1040. doi: 10.7567/1347-4065/ab079f
18. Peng M, Yin X, Tanner PA, et al. Site Occupancy Preference, Enhancement Mechanism, and Thermal Resistance of Mn<sup>4+</sup> Red Luminescence in Sr<sub>4</sub>Al<sub>14</sub>O<sub>25</sub>: Mn<sup>4+</sup> for Warm WLEDs. *Chemistry of Materials*. 2015; 27(8): 2938–2945. doi: 10.1021/acs.chemmater.5b00226
19. Wu T, Lin Y, Zhu H, et al. Multi-function indoor light sources based on light-emitting diodes-a solution for healthy lighting. *Optics Express*. 2016; 24(21): 24401–24412. doi: 10.1364/oe.24.024401
20. Zhu F, Lin Y, Huang W, et al. Multi-primary human-centric lighting based on the optical power ratio and the CCT super-smooth switching algorithms. *Building and Environment*. 2023; 228: 109880. doi: 10.1016/j.buildenv.2022.109880
21. Zhan X, Wang W, Chung HSH. A Novel Color Control Method for Multicolor LED Systems to Achieve High Color Rendering Indexes. *IEEE Transactions on Power Electronics*. 2020; 8: 136498.
22. Saw YJ, Kalavally V, Tan CP. The Spectral Optimization of a Commercializable Multi-Channel LED Panel with Circadian Impact. *IEEE Access*. 2020; 8: 136498–136511. doi: 10.1109/access.2020.3010339
23. Nie J, Wang Q, Dang W, et al. Tunable LED Lighting with Five Channels of RGCWW for High Circadian and Visual Performances. *IEEE Photonics Journal*. 2019; 11(6): 1–12. doi: 10.1109/jphot.2019.2950834
24. Stevens RG. Artificial Lighting in the Industrialized World: Circadian Disruption and Breast Cancer. *Cancer Causes & Control*. 2006; 17(4): 501–507. doi: 10.1007/s10552-005-9001-x
25. Wada K, Nagata C, Nakamura K, et al. Light exposure at night, sleep duration and sex hormone levels in pregnant Japanese women. *Endocrine Journal*. 2012; 59(5): 393–398. doi: 10.1507/endocrj.ej11-0325
26. Royer MP. Tutorial: Background and Guidance for Using the ANSI/IES TM-30 Method for Evaluating Light Source Color Rendition. *LEUKOS*. 2021; 18(2): 191–231. doi: 10.1080/15502724.2020.1860771
27. Han Z, Zhang Z, Liu K, et al. Spectral optimization of trichromatic white LEDs based on age of lighting user and application scene. *Optics Express*. 2023; 31(7): 11624–11632. doi: 10.1364/oe.485523
28. Cerpentier J, Meuret Y. Fundamental Spectral Boundaries of Circadian Tunability. *IEEE Photonics Journal*. 2021; 13(4): 1–5. doi: 10.1109/jphot.2021.3098903
29. Sun J, Zhang JW. Design of LED Light Source for Uniform Illumination in Large Area. *Applied Mechanics and Materials*. 2013; 401–403: 465–468. doi: 10.4028/www.scientific.net/amm.401-403.465
30. Davis W. Color quality scale. *Optical Engineering*. 2010; 49(3): 033602. doi: 10.1117/1.3360335